J. Biochem. **139**, 847–855 (2006)
doi:10.1093/jb/mvj103

Theoretical Study on Charge-Transfer Interaction between Acyl-CoA Dehydrogenase and 3-Thiaacyl-CoA Using Density Functional Method

Takeyuki Tanaka[1,*,†], Haruhiko Tamaoki[2,*], Yasuzo Nishina[3], Kiyoshi Shiga[3], Takashi Ohno[1] and Retsu Miura[2]

[1]Department of Biosystems Science, Graduate School of Science and Technology, Kobe University, 1-1 Rokodai-cho, Nada-ku, Kobe 657-8501; and Departments of [2]Molecular Enzymology and [3]Molecular Physiology, Graduate School of Medical Sciences, Kumamoto University, 1-1-1 Honjo, Kumamoto 860-8556

Received October 19, 2005; accepted March 9, 2006

Acyl-CoA dehydrogenase forms a complex with a substrate analog, 3-thiaacyl-CoA, exhibiting a charge-transfer (CT) band. The structure of a complex model of oxidized lumiflavin with deprotonated 3-thiabutanoate ethylthioester designed for the above CT complex was fully optimized by means of density functional theory (DFT), the spatial arrangement being similar to the corresponding X-ray structure reported previously. The electrostatic interaction between flavin and an anionic ligand, therefore, plays a major role in determination of the arrangement of the CT complex. When the excitation energies and oscillator strengths for the optimized structures of complex models including oxidized 8-substituted lumiflavins were calculated, the obtained wavelengths correlated well with observed values reported. Subsequently, we carried out DFT calculations for new complex models redesigned for complexes of oxidized 8-substituted FADs with an anionic ligand by introducing hydrogen bonds at the carbonyl group of the ligand with the 2′-hydroxyl group of the N10-ribityl of FAD and with the main-chain amide group of Glu376. The CT absorbing wavelengths of the new complex models exhibited better correlation with those observed previously. Consequently, comparison of substituent effects on the DFT calculations for the complex models will lead to a deeper understanding of the CT interaction and the effect of the hydrogen-bonding interaction on the CT framework.

Key words: acyl-CoA dehydrogenase, charge-transfer, density functional theory, flavin, hydrogen bond.

Abbreviations: ACD, acyl-CoA dehydrogenase; CT, charge-transfer; DFT, density functional theory; TD-DFT, time-dependent density functional theory; MCAD, medium-chain acyl-CoA dehydrogenase.

The acyl-CoA dehydrogenases (ACDs) comprise a family of flavoenzymes that catalyze the dehydrogenation of acyl-CoA to the corresponding *trans*-2-enoyl-CoA in the first step of the mitochondrial β-oxidation cycle (*1*, *2*). The dehydrogenation reaction consists of two processes; the abstraction of α-proton by a catalytic base and the transfer of β-hydride to oxidized flavin, as shown in Fig. 1A. The two processes proceed either in a stepwise manner with α-proton abstraction preceding β-proton transfer or in a concerted manner. Which reaction pathway is used depends on the member of the ACD family, type of substrate, or pH of the medium (*3*). According to the crystal structure (*4*) of medium-chain acyl-CoA dehydrogenase (MCAD) with a substrate, the carbonyl group of the substrate interacting with the flavin ring is hydrogen-bonded to the main-chain amide group of Glu376 and to the 2′-hydroxyl group of the N(10)-ribityl of FAD. These hydrogen bonds play an important role in the dehydrogenation reaction (*5*).

It is known that MCAD binds substrate analogs such as 3-thiaacyl-CoA and 3-ketoacyl-CoA and that the complexes give rise to a charge-transfer (CT) absorption band in a long-wavelength region (*6*–*8*). The above CT complex is regarded to reflect one of the metastable states in the dehydrogenation reaction, as shown in Fig. 1B. We recently reported the crystal structure (PDB-ID: 1UDY) of MCAD with deprotonated 3-thiaoctanoyl-CoA, abbreviated as MCAD-3-thia-C8-CoA (*9*). Only analysis involving X-ray crystallography combined with density functional theory (DFT) calculations, we concluded that the 3-thiaoctanoyl-CoA is deprotonated by COO^- of Glu376 and the negative charge of the ligand is delocalized to the oxidized flavin ring. We also demonstrated that the CT interaction plays an important role in determination of the arrangement of the flavin ring with the anionic ligand in the ACD active site. Spectroscopic studies of complexes between MCADs reconstituted with 8-substituted flavins and some substrate analogs showed that the CT interaction, in concert with the hydrogen bonds at the carbonyl

*To whom correspondence should be addressed. Phone/Fax: +81-89-946-9587, E-mail: putaro@protein.osaka-u.ac.jp (T.Tanaka); Phone: +81-96-373-5063, Fax: +81-96-373-5066, E-mail: harr@gpo.kumamoto-u.ac.jp (H.Tamaoki).
†Present address: Integrated Center for Sciences, Ehime University, 3-5-7 Tarumi, Matsuyama, Ehime 790-8566.

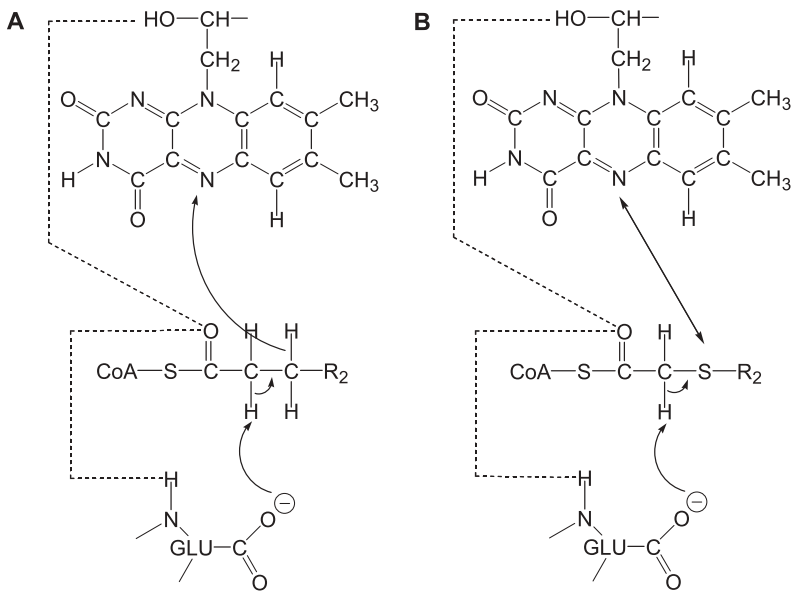

Fig. 1. **Scheme of dehydrogenation reaction (A) of a substrate and charge-transfer complex formation (B) of a substrate analog for MCAD.**

group of the ligand, lowers the pK_a value of the ligand (*10*). The DFT method supported the theoretical interpretation of the correlation between the wavelength of the CT band and the sum of the Hammet σ parameters (*11*) for the substituents at the 7- and 8-positions of the flavin ring.

DFT calculations of the α-proton abstraction (*12*) from a substrate (analogs) bound to ACD and the CT interaction (*13*) of ACD with the substrate (analog) have been performed. The latter suggested that the CT band could be reproduced by means of time-dependent DFT (TD-DFT) (*14*) with small basis sets. In general, a TD-DFT calculation with a small basis set cannot give results that coincide with those of a corresponding experiment (*15*, *16*). Care should be taken in calculating the CT absorption band because of the small energy gap, although the excitation energies of flavin-related molecules (*17*, *18*) determined on TD-DFT calculation agree with the experimental values with moderately large basis sets.

In the present study, the structures of complex models designed for MCAD-3-thia-C8-CoA with and without hydrogen bonds were optimized by DFT calculations with some large basis sets ignoring any solvent effect and their CT absorption bands were calculated by TD-DFT in order to determine the effect of the hydrogen bonds on the CT interaction. After confirming the validity of the TD-DFT calculation for the CT band with the large basis sets, DFT calculations for the models designed for the complexes between MCADs reconstituted with 8-substituted flavins and 3-thiaacyl-CoA were performed, the results being compared with the corresponding experimental results (*10*). The substituent effects on the detailed structures of the CT complexes were analyzed theoretically on the basis of the DFT calculations; these effects cannot be observed experimentally but can only be analyzed by means of calculations. Finally, we report the relationship between the acyl-CoA dehydrogenation reaction and the results of the DFT calculations.

EXPERIMENTAL PROCEDURES

Two calculation models designed for MCAD-3-thia-C8-CoA (*9*, *10*) were used in this work. One model is a simplified one; a complex of oxidized lumiflavin (Fig. 2A) with deprotonated 3-thiabutanoate ethylthioester (Fig. 2C). The other model is a hydrogen-bonding model obtained by extending the simplified model to include the hydrogen bonds of the carbonyl group of the substrate analog with the 2′-hydroxyl group of the N10-ribityl and with the main-chain amide of Glu376. In the hydrogen-bonding model, the model compound, oxidized 2′-OH-flavin (Fig. 2B), was used for FAD and *N*-methylacetamide (*19*) (Fig. 2D), which represents the main-chain model corresponding to the Glu376 main-chain amide. The 2′-hydroxyl and amide groups were arranged so as to hydrogen-bond with the carbonyl group of the ligand. If the hydrogen-bonding model is energetically stabilized by the hydrogen-bond formations, the spatial arrangements of the two groups should be decided uniquely.

All DFT calculations were carried out with the Gaussian 03 program (*20*) on DELL Precision Workstation 450 machines. The structures of complex models were fully optimized using B3LYP functional (*21*, *22*) with the 6-31G(d), 6-311G(d), 6-311+G(d), 6-311+G(d,p), or 6-311+G(2d,p) basis set. The wavelengths and oscillator strengths for the optimized structures were calculated at the same calculation level as for optimization on the basis of the TD-DFT. At the limit of vertical transition, only 30 singlet states were calculated for excited states. Electronic absorption spectra of complex models were generated from the calculated values assuming that each band is a Gaussian waveform with a bandwidth of 3,000 cm^{-1}.

RESULTS

Structure and Electronic Absorption Spectrum of a Simplified Model—The structure of a complex of oxidized lumiflavin (Fig. 2A) with deprotonated 3-thiabutanoate ethylthioester (Fig. 2C) was fully optimized with B3LYP functional and the 6-311G(d) basis set. This complex model is designated as a simplified model. The optimized structure is shown in Fig. 3. The thioester plane is slightly tilted above the flavin ring plane and the S(3) atom of the ligand is located above N5 of the flavin at an atomic distance of

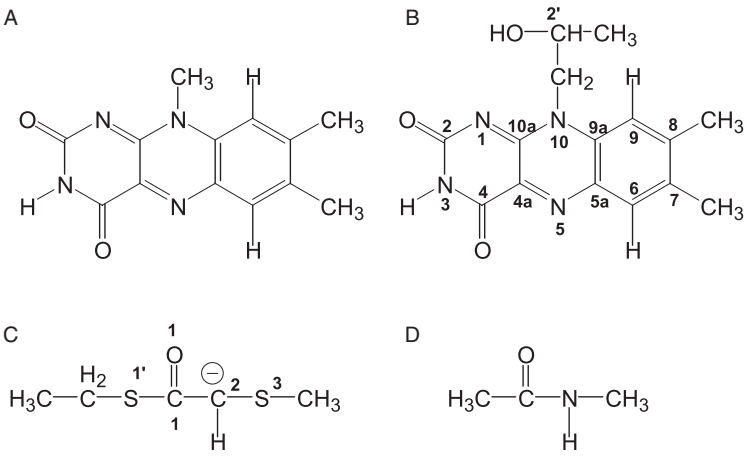

Fig. 2. **Chemical structures of molecules used for the simplified and hydrogen-bonding models: lumiflavin (A), 2′-OH-flavin (B), 3-thiabutanoate ethylthioester (C), and *N*-methylacetamide (D).**

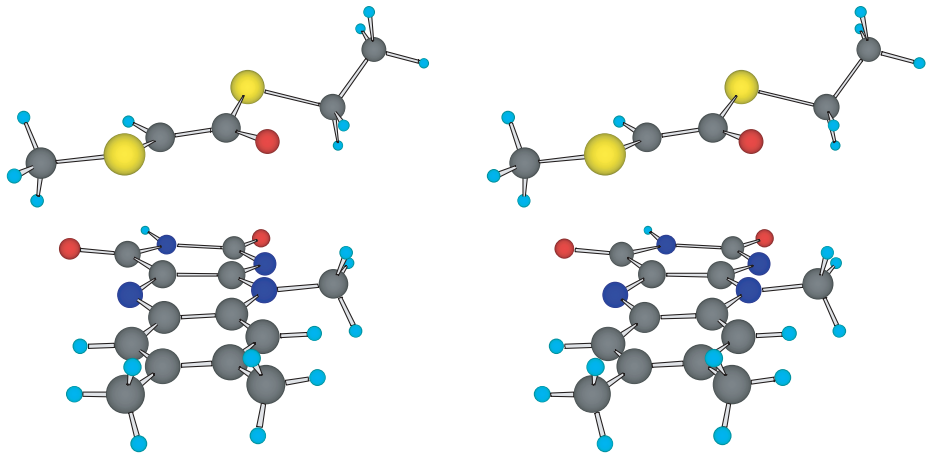

Fig. 3. **Stereoscopic view of stereochemical structures for the simplified model with B3LYP/6-311G(d).**

3.121 Å. (The numbering for the ligand and flavin atoms is given with in and without parenthesis, respectively, throughout the text.) The short distance of S(3)-N5 suggests that the β-hydride of the substrate can be transferred to the N5 atom of the flavin on the dehydrogenation of acyl-CoA (Fig. 1A). The atomic distances for C(2)-C4a and C(1)-C10a were calculated to be 2.898 and 3.128 Å, respectively. However, they are shorter than the corresponding atomic distances, 3.71 and 3.74 Å, respectively, which are the average values observed for the tetramer of the MCAD-3-thia-C8-CoA crystal structure (*9*). The difference may have arisen from basis-set dependence, incomplete design of the complex, the ignoring of the solvent effect, *etc.*

For the simplified model, the wavelengths and oscillator strengths were calculated by TD-DFT. The wavelength and oscillator strength of the CT absorption band of B3LYP/6-311G(d) were calculated to be 696 nm and 0.2417, respectively. The calculated wavelength is shorter than the 808 nm observed for MCAD-3-thia-C8-CoA (*7*). Taking into consideration that the shorter wavelength is ascribed to the small basis set, we recalculated the structure and the electronic absorption for the simplified model by TD-DFT with various basis sets. The simulated spectra are shown in Fig. 4. The spectral features of the simulation are the same but depend on the basis set. The CT absorption band of the simplified model was calculated to be 747 nm with B3LYP/6-311+G(2d,p), the highest basis set used in this work, and its calculated oscillator strength was 0.1953. Note that the wavelength difference between B3LYP/6-311G(d) and B3LYP/6-311+G(2d,p) is 51 nm. The atomic distances of C(2)-C4a and C(1)-C10a calculated with B3LYP/6-311+G(2d,p) were 2.970 and 3.188 Å, respectively. The calculated values with the large basis set are closer to those of the MCAD-3-thia-C8-CoA crystal structure than those with the 6-311G(d) basis set. The overall arrangement of the model agreed with the corresponding crystal structure except for a slight difference in the atomic distance.

Electronic absorption spectra of complexes between MCADs reconstituted with artificial FADs, *i.e.*, 8-cyano-, 7,8-dichloro-, 8-chloro, 8-methoxy-, and 8-amino-FADs, and 3-thiaoctanoyl-CoA have been measured (*10*). DFT calculations for simplified models designed for the complexes were carried out with B3LYP/6–311G(d) taking advantage of the computational efficiency. The abbreviations for the simplified models designed for the complexes between MCADs reconstituted with 8-cyano-, 7,8-dichloro-, 8-chloro, 8-methyl-, 8-methoxy-, and 8-amino-FADs, and 3-thiaoctanoyl-CoA are cyano, dichloro, chloro, normal, methoxy, and amino, respectively. The Cartesian coordinates of the optimized structures are given in Table S1 of

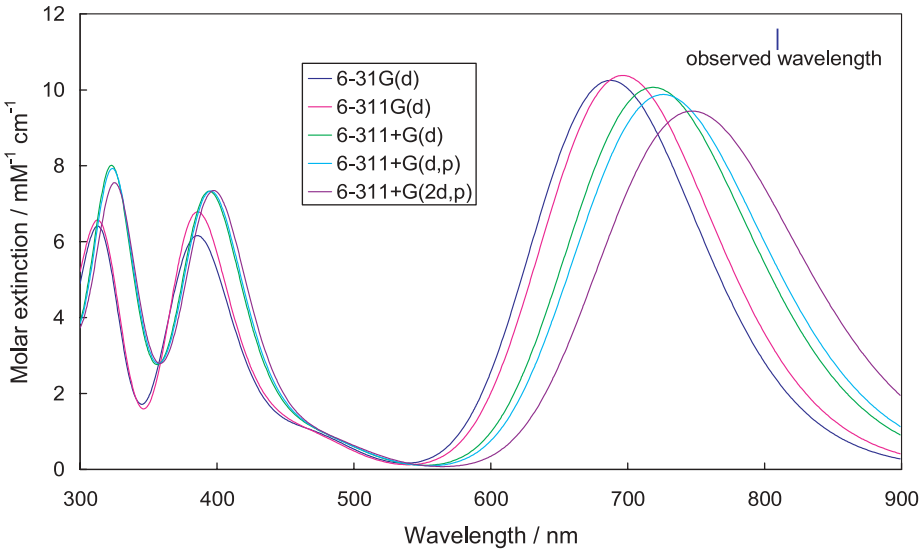

Fig. 4. **Dependence of simulated electronic absorption spectra of the simplified models on the basis sets, 6-31G(d), 6-311G(d), 6-311+G(d), 6-311+G(d,p), and 6-311+G(2d,p), using B3LYP functional.** The observed absorbing wavelength of the CT band (Ref. *10*) is represented as a bar.

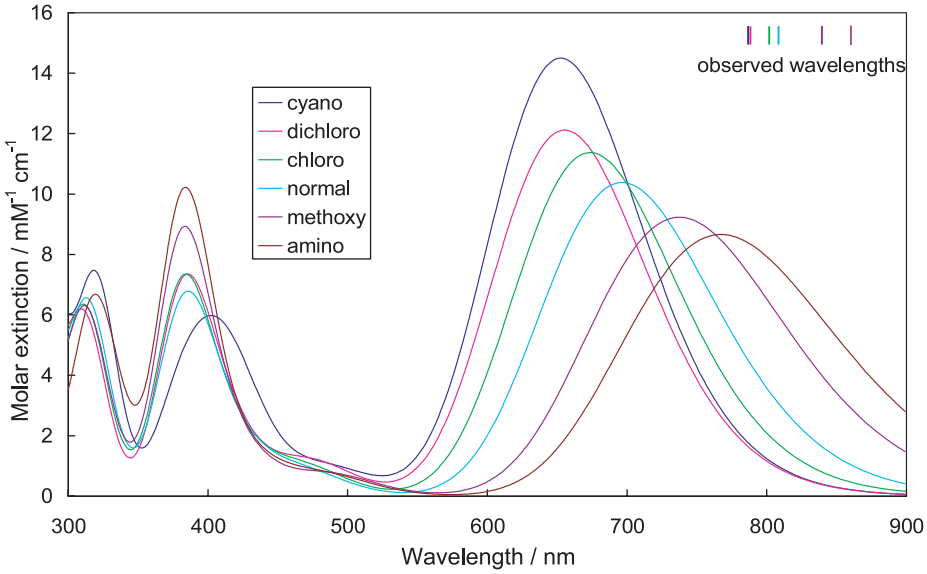

Fig. 5. **Simulated electronic absorption spectra of the simplified models including 8-substituted flavins with B3LYP/6-311G(d).** cyano, 8-cyano-; dichloro, 7,8-chloro-; chloro, 8-chloro-; normal, 8-methyl-; methoxy, 8- methoxy-; and amino, 8-amino-lumiflavins. The observed absorbing wavelengths of the CT band (Ref. *10*) are represented as bars.

the supplementary material. Although the calculated wavelengths are shorter than those observed, the CT absorption bands of the simplified models were successfully reproduced with B3LYP/6-311G(d), as shown in Fig. 5. The calculated wavelengths of the CT bands show good correlation with the observed ones, although the CT bands may all be calculated at a shorter wavelength, by 51 nm, due to the small basis set. Accordingly, the simplified models sufficiently reflect the substituent effect of flavin at the 8-position in MCAD-3-thia-C8-CoA on the CT band.

Structure and Electronic Absorption Spectrum of a Hydrogen-Bonding Model—The structure (Fig. 6) of the complex of oxidized 2′-OH-flavin (Fig. 2B) with an anionic 3-thiabutanoate ethylthioester (Fig. 2C) and *N*-methylacetamide (Fig. 2D) was fully optimized with B3LYP/6-311G(d), and exhibited a CT band at 785 nm with TD-DFT at the same calculation level. In the case of a hydrogen-bonding model, we did not select the large basis set, 6-311+G(2d,p), because of the great computation time. It was ascertained that the spatial arrangements of the 2′-hydroxyl and amide groups are only determined by the hydrogen bonding. The calculated atomic distances for C(2)–C4a and C(1)–C10a were 3.011 and 3.381 Å, respectively. The introduced hydrogen bonds reduced the deviation from the atomic distances of MCAD-3-thia-C8-CoA in comparison with the simplified model. Moreover, the distances of the two hydrogen bonds at the carbonyl group of the substrate analog with the nitrogen atom of *N*-methylacetamide and with the oxygen atom of the N10-ribityl were calculated to be 2.935 and 2.690 Å, respectively. The corresponding average atomic distances for the tetramer of MCAD-3-thia-C8-CoA are 3.13 and 2.66 Å. The hydrogen-bonding strengths, therefore, are in good agreement with those in the hydrogen-bonding model. Taking into consideration that a small basis set, 6-311G(d), gives rise to a shorter CT-wavelength, by 51 nm, than that obtained with a large basis set, 6-311+G(2d,p), TD-DFT calculation with B3LYP/6-311+G(2d,p) is expected to give the wavelength of 836 nm for the CT absorption

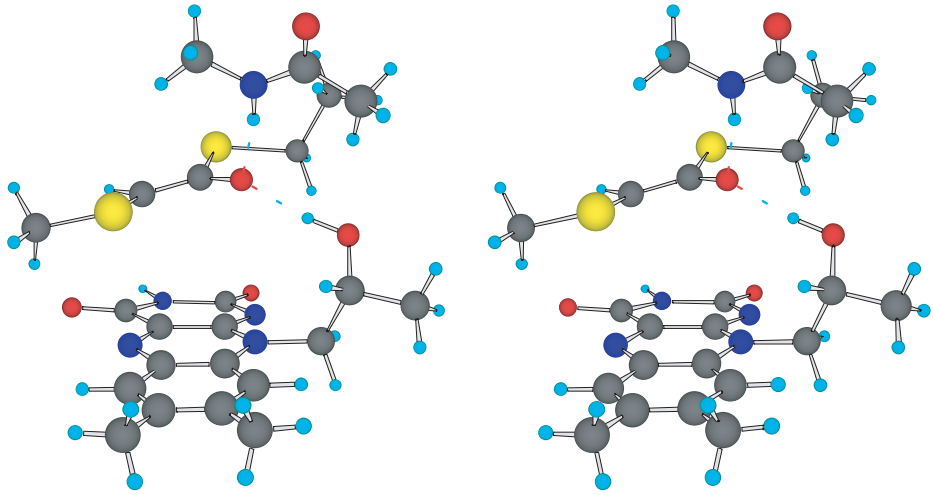

Fig. 6. **Stereoscopic view of stereochemical structures for the hydrogen-bonding models with B3LYP/6-311G(d).**

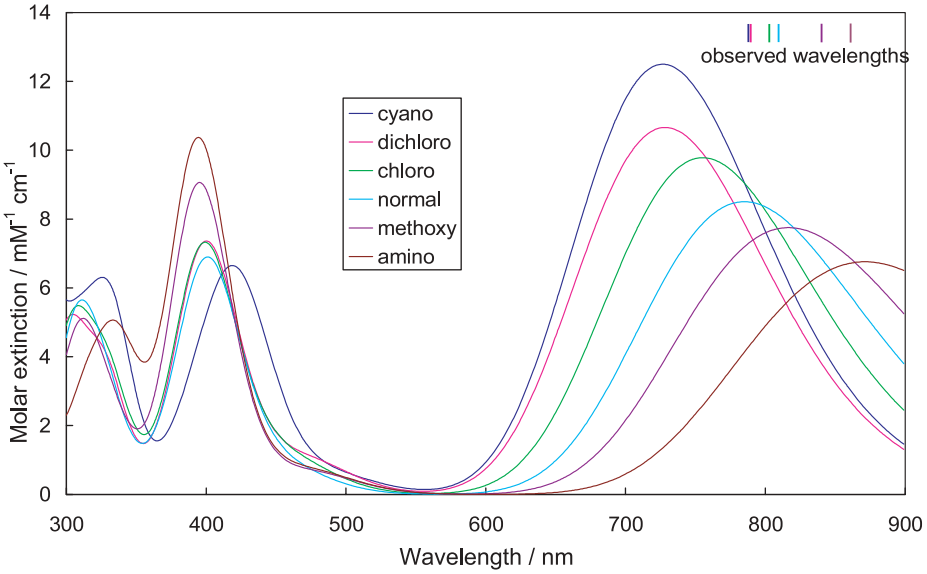

Fig. 7. **Simulated electronic absorption spectra of the hydrogen-bonding models including 8-substituted flavins with B3LYP/6-311G(d).** The abbreviations, cyano, dichloro, chloro, normal, methoxy, and amino, correspond to 2′-OH-flavin derivatives (B in Fig. 2) with substituents at the 7- and 8-positions. The observed absorbing wavelengths of the CT band (Ref. *10*) are represented as bars.

band. This expected wavelength is slightly longer than the observed one, 808 nm. The slight disagreement of the CT band may arise from overestimation of the hydrogen-bonding strength with *N*-methylacetamide. Regardless of the slight difference, the DFT calculation with the large basis sets reflects the CT interaction in the experimental electronic spectrum even though no solvent effects were considered, as reported previously (*13*).

DFT calculations for hydrogen-bonding models of cyano, dichloro, chloro, normal, methoxy, and amino in the same way as for simplified models were carried out with B3LYP/6-311G(d). The Cartesian coordinates of the optimized structures are given in Table S1 of the supplementary material. The simulated spectra are shown in Fig. 7. The tendency of the CT absorption bands for the hydrogen-bonding models with respect to wavelength and oscillator strength is coincident with that of the simplified models (Fig. 5). It was found that the substituent effect on the CT interaction is independent of the formation of the hydrogen bonds and the effect of the hydrogen bonds on the CT interaction is ~83 nm (~1530 cm^{-1} in wavenumber).

DFT calculations of models designed for the complexes of 2′-deoxy-8-chloro-FAD or 2′-deoxy-8-cyano-FAD with the 3-thiaoctanoyl-CoA were also performed. The structures of the complexes of 8-chloro- or 8-cyano-lumiflavin with an anionic 3-thiabutanoate ethylthioester and with *N*-methylacetamide were fully optimized with B3LYP/6-311G(d), and their wavelengths and oscillator strengths were calculated by TD-DFT at the same level. The calculated wavelengths and oscillator strengths of the complex models including 8-chloro- and 8-cyano-flavin were 724 nm (0.2122) and 690 nm (0.2801), respectively, the calculated oscillator strength being given in parenthesis. The calculated wavelengths are not in good agreement with the observed values, 770 and 747 nm, respectively, but the differences from the corresponding hydrogen-bonding models, 31 and 37 nm, are close to the experimental values, 32 and 41 nm (*10*), respectively. This suggests that the hydrogen-bonding model suffices to reflect the hydrogen bond at the carbonyl group of the ligand with the 2′-ribityl group of the N10-ribityl in MCAD-3-thia-C8-CoA.

DISCUSSION

The Charge-Transfer Absorption Bands of the Simplified and Hydrogen-Bonding Models—Figure 8

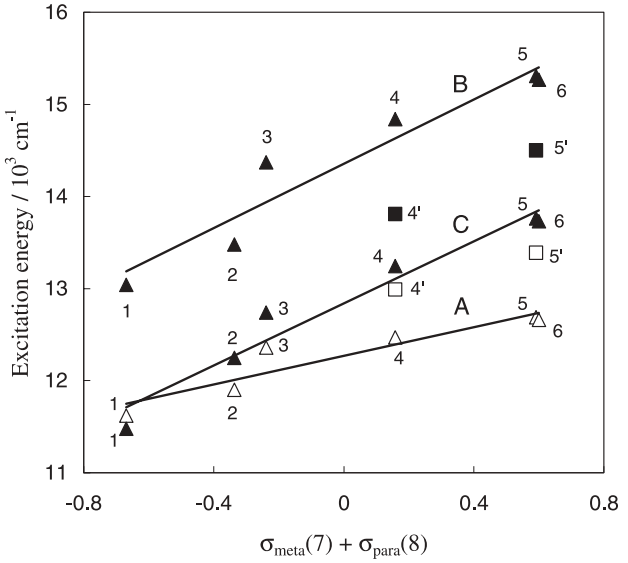

Fig. 8. **Correlation between the excitation energies of the CT absorption bands for the complexes including 8-substituted flavins with 3-thiaacyl-CoA and the sum of the Hammet σ parameters for the substituents at the 7- and/or 8-positions.** For observed (A) and calculated values for the simplified (B) and hydrogen-bonding models (C), least-squares fitting lines were calculated. Data numbering: 1, 8-amino-; 2, 8-methoxy-; 3, 8-methyl-; 4, 8-chloro-; 5, 8-cyano-; 6, 7,8-dichloro-; 4′, 2′-deoxy-8-chloro-; 5′, 2′-deoxy-8-cyano-flavins. Solid and open symbols represent calculated and observed data, respectively.

shows the correlation between the excitation energies of the CT absorption bands for the complexes including the 8-substituted flavins and the sum of the Hammet σ parameters for the substituents at the 7- and/or 8-positions. The features of the calculated values for the simplified and hydrogen-bonding models are similar to those of the observed ones. The similarity substantiates the validity of the two calculation models used for the DFT calculations. The slopes of the least-squares fitting lines of the two calculations are slightly different from that observed but are coincident with each other. The coincidence of the slopes suggests that the substituent effect is independent of the hydrogen-bonding and that the simplified model is sufficient for investigating the substituent effect of MCAD-3-thia-C8-CoA without the use of the hydrogen-bonding model, which is too heavy to compute. The difference in the slopes may be ascribed to the hydrogen-bonding interactions at other positions of flavin, which are not taken into account in this work. In other words, the electron-accepting ability of the flavin ring may be maintained via the hydrogen bonds with surrounding amino acids, which might act as a means of feedback in the active site when the electron-withdrawing ability of the substituent in the flavin is too high. In addition, the effect of the hydrogen bond at the carbonyl group of the ligand with and without the 2′-hydroxyl group of N10-ribityl on the CT interaction is reproduced in the DFT calculation. Note that the data points for 4′ and 5′ in Fig. 8 are for 2′-deoxy flavin derivatives in which the ligand C(1)=O(1) is only hydrogen-bonded with the amide hydrogen of Glu376 or *N*-methylacetamide. As previously stated under Results, the hydrogen-bonding model is sufficient to reflect the hydrogen bond with the 2′-hydroxyl group of N10-ribityl and can reflect the effect of the hydrogen bond with the main-chain amide group of Glu376 on the CT interaction. Consequently, the good agreement of the DFT calculations with the experimental results, as shown for the 2′-deoxy substituents in Fig. 8, confirms the validity of the calculated values obtained for the complex model.

Regarding the validation of the DFT calculations, one can estimate the contribution of the hydrogen bond at the carbonyl group of the ligand with the main-chain amide group to the CT interaction. The differences in wavelengths for the complex models of 8-cyano- and 8-chloro-lumiflavin with 3-thiabutanoate ethylthioester and *N*-methylacetamide from the corresponding simplified models are 37 and 50 nm, respectively. These values are comparable to the contributions, 37 and 31 nm, respectively, of the hydrogen bond with the 2′-hydroxyl group of N10-ribityl. Since such values cannot be determined experimentally, they are very valuable and theoretically meaningful quantities only obtainable by such calculations as those carried out in this study.

Substituent Effect in the Simplified Model—The stabilization energies, bond lengths, atomic distances, and CT band parameters of the simplified models obtained with B3LYP/6-311G(d) are summarized in Table 1. Since all the stabilization energies are negative, the flavin and ligand are energetically stabilized due to the complex formation. The absolute value of the stabilization energy, $|\Delta E|$, on the CT interaction increases in the order of cyano > dichloro > chloro > methoxy > amino. C(1)-C(2), C(1)-S(1′), and C(2)-S(3) exhibit the largest displacement among all the bonds in the flavin and the ligand. Comparison of the bond lengths of C(1)=O(1) for the simplified models with those for hydrogen-bonding models will be discussed in the subsequent section. It is noteworthy that the bond lengths of C(1)-C(2), C(1)-S(1′), and C(2)-S(3) of the ligand change appreciably due to the substituent effect via the CT interaction between the substituted flavins and the ligand. The smaller the $|\Delta E|$, the shorter the bond lengths of C(1)-C(2), and the longer the bond lengths of C(1)-S(1′), C(1)=O(1), and C(2)-S(3). These results reveal that the bond order of C(1)-C(2) of the anionic ligand decreases with increasing electron-accepting ability of the flavin ring (bond order: cyano < dichloro < chloro < methoxy < amino), and the distortion through C(1)-C(2) may be absorbed by compensatory displacement in the neighboring bonds of C(1)-S(1′), C(1)=O(1), and C(2)-S(3). For the atomic distances shown in Table 1, the smaller the $|\Delta E|$, the longer all the distances except for C(1)-C10a and O(1)-C10a of dichloro. The exception indicates that the electron-withdrawing ability of the 7-chloro-substituent strongly affects the atomic orbital of C10a in the flavin ring. For the CT band parameters, the smaller the $|\Delta E|$, the smaller the wavenumber and the smaller the oscillator strength when the wavelength is transformed into the wavenumber. Namely, the CT band parameters exhibit good correlation with the stabilization energies.

Substituent Effect in the Hydrogen-Bonding Model—The stabilization energies, bond lengths, atomic distances, and CT band parameters of the hydrogen-bonding models obtained with B3LYP/6-311G(d) are summarized in Table 2. All the magnitudes of the stabilization energies for the hydrogen-bonding models are larger than those for

Table 1. **Stabilization energies, bond lengths, atomic distances, and CT band parameters of the simplified models including 8-substituted flavins with B3LYP/6-311G(d).**

	cyano	dichloro	chloro	normal	methoxy	amino
Stabilization energy / kcal mol^{-1}						
ΔE*[1]	–21.22	–19.35	–14.83	–10.33	–8.77	–6.61
Bond length/Å						
C(1)-C(2)	1.409	1.406	1.402	1.398	1.395	1.393
C(1)-S(1′)	1.866	1.871	1.877	1.884	1.888	1.892
C(1)=O(1)	1.229	1.230	1.231	1.233	1.234	1.235
C(2)-S(3)	1.747	1.751	1.754	1.759	1.763	1.765
Atomic distance/Å						
C(1)-C10a	3.099	3.096	3.113	3.128	3.138	3.145
O(1)-C10a	3.197	3.191	3.201	3.206	3.210	3.206
C(2)-C4a	2.795	2.820	2.856	2.898	2.942	2.984
S(3)-N5	3.050	3.057	3.084	3.121	3.175	3.204
CT band parameter						
Observed wavelength*[2]/nm	788	789	802	808	840	861
Calculated wavelength/nm	653	655	674	696	737	767
Calculated oscillator strength	0.300	0.251	0.235	0.215	0.191	0.179

*[1]ΔE = E(complex) – E(8-substituted lumiflavin) – E(3-thiabutanoate ethylthioester). *[2]The observation was reported in Ref. *10*.

Table 2. **Stabilization energies, bond lengths, atomic distances, and CT band parameters of the hydrogen-bonding models including 8-substituted flavins with B3LYP/6-311G(d).**

	cyano	dichloro	chloro	normal	methoxy	amino
Stabilization energy/kcal mol^{-1}						
ΔE*[1]	–39.59	–38.38	–34.51	–31.10	–29.78	–28.05
$\Delta\Delta E$*[2]	–18.37	–19.03	–19.68	–20.77	–21.01	–21.44
Bond length/Å						
C(1)-C(2)	1.390	1.386	1.383	1.379	1.376	1.374
C(1)-S(1′)	1.834	1.837	1.842	1.842	1.845	1.847
C(1)=O(1)	1.259	1.262	1.263	1.267	1.269	1.271
C(2)-S(3)	1.750	1.753	1.757	1.763	1.766	1.769
Atomic distance/Å						
C(1)-C10a	3.330	3.322	3.369	3.381	3.397	3.427
O(1)-C10a	3.469	3.461	3.510	3.510	3.526	3.548
C(2)-C4a	2.902	2.919	2.963	3.011	3.042	3.092
S(3)-N5	3.052	3.068	3.102	3.149	3.185	3.237
O(1)-H(2′-ribityl)	1.739	1.728	1.726	1.712	1.704	1.696
O(1)-H(*N*-methylacetamide)	1.964	1.957	1.952	1.925	1.915	1.910
CT band parameter						
Observed wavelength*[3]/nm	788	789	802	808	840	861
Calculated wavelength/nm	727	728	755	785	816	871
Calculated oscillator strength	0.259	0.221	0.202	0.176	0.160	0.140

*[1]ΔE = E(complex) – E(8-substituted 2′-OH-flavin) – E(3-thiabutanoate ethylthioester) – E(*N*-methylacetamide). *[2]$\Delta\Delta E$ = ΔE(hydrogen-bonding model) – ΔE(simplified model). *[3]The observation was reported in Ref. *10*.

the simplified models. This suggests that the hydrogen-bond formations contribute to the energetic stabilization as well as the CT formation.

Moreover, the energetic stability on the hydrogen bonding is represented by the absolute difference between ΔE (hydrogen-bonding model) and ΔE (simplified model), $|\Delta\Delta E|$, which increases in the order of cyano < dichloro < chloro < methoxy < amino. The increases and decreases of the bond lengths, atomic distances, and CT band parameters relative to the stabilization energy are the same as those for the simplified models. C(1)=O(1) is affected by the hydrogen bonds with *N*-methylacetamide and the 2′-hydroxyl group, and the bond length is longer with greater $|\Delta\Delta E|$. This was ascertained from the atomic distances of the hydrogen bonds. Namely, the greater the $|\Delta\Delta E|$, the shorter the atomic distances of O(1)-H(2′-ribityl) and O(1)-H(*N*-methylacetamide). The change in the hydrogen-bonding strength gives rise to the large displacement of the bond length of C(1)=O(1). Therefore, the most different property between the simplified and hydrogen-bonding models is the bond length of C(1)=O(1).

Effect of the Hydrogen Bonds on the Charge-Transfer Interaction—As can be seen in Fig. 6, the hydrogen bonds at the carbonyl group of the ligand with the 2′-hydroxyl group of the N10-ribityl and with the amide group of *N*-methylacetamide are seemed to anchor the ligand on the flavin ring. However, since the ligand is bound to the flavin ring without hydrogen bonds in the simplified

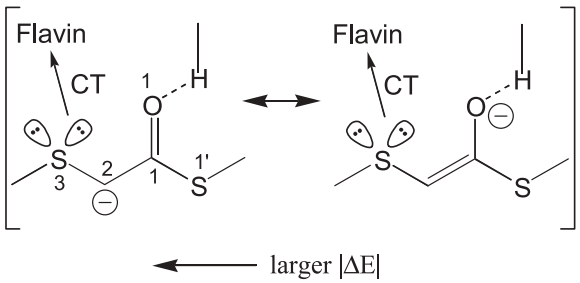

Fig. 9. **Relationship between the CT and hydrogen-bonding interactions *via* the bond order of C(1)=O(1) and C(1)-C(2).**

model and takes the same spatial arrangement as that in the hydrogen-bonding model, the hydrogen bonds are not necessary to fix the spatial arrangement of the ligand. In addition, the longer wavelength of the CT absorption band and the longer atomic distances for the hydrogen-bonding model than those for the simplified model reveal that the hydrogen bonds weaken the CT interaction. The role of the hydrogen bonds is to lower the pK_a of the ligand. This is deduced from the following. The hydrogen bonds lengthen C(1)=O(1) and shorten C(1)-C(2) in order to delocalize the negative charge on the C(2) atom of the anionic ligand. As a result, the pK_a at the C(2) atom drops. The relationship between the CT and hydrogen-bonding interactions via the bond order of C(1)=O(1) and C(1)-C(2) is schematically illustrated in Fig. 9. It is deduced from the energetic stabilization, $\Delta\Delta E$, in Table 2 that the CT and hydrogen-bonding interactions have a greater effect on lowering of the pK_a than the CT interaction without hydrogen bonds because the CT complex becomes energetically stable state due to the interactions even though the hydrogen bonds slightly weaken the CT interaction.

Acyl-CoA Dehydrogenation Reaction—The stabilization energies of the complex models are associated with the stability of the complex of MCAD with the substrate (analog) after the abstraction of the α-proton in the ligand. The CT and hydrogen-bonding interactions promote the α-proton abstraction since the two interactions make the metastable state stabilized energetically. Moreover, the substituent at the 8-position of FAD with an electron-withdrawing group contributes to the promotion of the α-proton abstraction, judging from ΔE in Tables 1 and 2. In addition, the atomic distances of S(3)-N5 for the complex models indicate the possibility of β-hydride transfer in the acyl-CoA dehydrogenation reaction. After a substrate (analog) binds to the active site, the α-proton is abstracted by Glu376-COO^- accompanying β-hydride transfer to flavin in the case of the substrate and CT complex formation in the case of 3-thiaoctanoyl-CoA. Therefore, the β-hydride transfer and the CT complex formation can be regarded on the same mechanistic level. Hence, the CT interaction is a favorable measure of the β-hydride transfer. However, the hydrogen-bond formations weaken the CT interaction and lengthen the atomic distance of S(3)-N5, as can be seen in Tables 1 and 2. The disadvantage of the hydrogen bonds for the β-hydride transfer can be overcome by reconstituting the 8-substituted FAD with an electron-withdrawing group. For example, the difference in the atomic distances of S(3)–N5 for cyano between the simplified and hydrogen-bonding models is negligible, and the decrease in the stabilization energy for cyano is small when the hydrogen bonds are formed. Consequently, the 8-cyano substituent can better promote the dehydrogenation reaction than the others.

CONCLUSIONS

The CT interaction of an ACD with a substrate analog is mainly ascribed to the electrostatic interaction of a flavin ring with an anionic ligand based on DFT calculations of the complex models. The DFT calculations of the hydrogen-bonding model strongly support that the energetic stabilization is due to the hydrogen bonds at the carbonyl group of the ligand with the main-chain amide group of Glu376 and with 2′-hydroxyl group of N10-ribityl. It is suggested that the hydrogen bonds affect the CT interaction. DFT analysis of the complexes including the 8-substituted flavins revealed that the CT interaction and the hydrogen bonding give rise to large displacement of the bond lengths not in the flavin but in the ligand. Additionally, the effect of the hydrogen bond at carbonyl group of the ligand with the main-chain amide group of Glu376 on the CT interaction can be estimated through DFT calculations; this effect cannot be observed experimentally but can be only estimated by means of calculation. It should be emphasized that DFT calculations can evaluate various interactions in the ACD system and can analyze them individually. DFT calculations will reveal hitherto undetected aspects and lead to a deeper understanding of the ACD dehydrogenation reaction.

Supplementary data are available at JB online.

This work was supported by a Grant-in-Aid for Science Research (No. 15607015) from the Japan Society for the Promotion of Science (JSPS).

REFERENCES

1. Grane, F.L., Mii, S., Hauge, J.G., Green, D.E., and Beinert, H. (1956) On the mechanism of dehydrogenase of fatty acyl derivatives of coenzyme A. I. The general fatty acylcoenzyme A dehydrogenase. *J. Biol. Chem.* **218**, 701–716
2. Ghisla, S. and Thorpe, C. (2004) Acyl-CoA dehydrogenases. A mechanistic overview. *Eur. J. Biochem.* **271**, 494–508
3. Engel, P.C. (1992) Acyl-CoA dehydrogenases in *Chemistry and Biochemistry of Flavoenzymes* (Müller, F., eds.) Vol. III, pp. 597–655, CRC Press, Boca Raton, Ann Arbor, London
4. Kim, J.-J.P., Wang, M., and Paschke, R. (1993) Crystal structures of medium-chain acyl-CoA dehydrogenase from pig liver mitochondria with and without substrate. *Proc. Natl. Acad. Sci. USA* **90**, 7523–7527
5. Engst, S., Vock, P., Wang, M., Kim, J.-J.P., and Ghisla, S. (1999) Mechanism of activation of acyl-CoA substrates by medium chain acyl-CoA dehydrogenase. Interaction of the thioester carbonyl with the flavin adenine dinucleotide ribityl side chain. *Biochemistry* **38**, 257–267
6. Thorpe, C. and Massey, V. (1983) Flavin analogue studies of pig kidney general acyl-CoA dehydrogenase. *Biochemistry* **22**, 2972–2978
7. Lau, S.-M., Brantley, R.K., and Thorpe, C. (1988) The reductive half-reaction in acyl-CoA dehydrogenase from pig kidney. Studies with thiaoctanoyl-CoA and oxaoctanoyl-CoA analogs. *Biochemistry* **27**, 5089–5095

8. Tamaoki, H., Nishina, Y., Shiga, K., and Miura, R. (1999) Mechanism for the recognition and activation of substrate in medium-chain acyl-CoA dehydrogenase. *J. Biochem.* **125**, 285–296
9. Satoh, A., Nakajima, Y., Miyahara, I., Hirotsu, K., Tanaka, T., Nishina, Y., Shiga, K., Tamaoki, H., Setoyama, C., and Miura, R. (2003) Structure of the transition state analog of medium-chain acyl-CoA dehydrogenase. Crystallographic and molecular orbital studies on the charge-transfer complex of medium-chain acyl-CoA dehydrogenase with 3-thiaoctanoyl-CoA. *J. Biochem.* **134**, 297–304
10. Nishina, Y., Sato, K., Tamaoki, H., Tanaka, T., Setoyama, C., Miura, R., and Shiga, K. (2003) Molecular mechanism of the drop in the p*K*a of a substrate analog bound to medium-chain acyl-CoA dehydrogenase. Implications for substrate activation. *J. Biochem.* **134**, 835–842
11. Edmondson, D.E. (1999) Electronic effects of 7 and 8 ring substituents as predictors of flavin oxidation-reduction potentials in *Flavins and Flavoproteins 1999* (Ghisla, S. Kroneck, P., Macheroux, P., and Sund, H., eds.) pp. 71–76, Rudolf Weber, Berlin
12. Bach, R.D., Thorpe, C., and Dmitrenko, O. (2002) C-H···carboxylate oxygen hydrogen bonding in substrate activation by acyl-CoA dehydrogenases. Synergy between the H-bonds. *J. Phys. Chem. B.* **106**, 4325–4335
13. Dmitrenko, O., Thorpe, C., and Bach, R.D. (2003) Effect of a charge-transfer interaction on the catalytic activity of acyl-CoA dehydrogenase. A theoretical study of the role of oxidized flavin. *J. Phys. Chem. B.* **107**, 13229–13236
14. Bauernschmitt, R. and Ahlrichs, R. (1996) Treatment of electronic excitations within the adiabatic approximation of time dependent density functional theory. *Chem. Phys. Lett.* **256**, 454–464
15. Wiberg, K.B., Stratmann, R.E., and Frisch, M.J. (1998) A time-dependent density functional theory study of the electronically excited states of formaldehyde, acetaldehyde and acetone. *Chem. Phys. Lett.* **297**, 60–64
16. Paddon-Row, M.N. and Shephard, M.J. (2002) A time-dependent density functional study of the singlet-triplet energy gap in charge-separated states of rigid bichromophoric molecules. *J. Phys. Chem. A.* **106**, 2935–2944
17. Neiss, C., Saalfrank, P., Parac, M., and Grimme, S. (2003) Quantum chemical calculation of excited states of flavin-related molecules. *J. Phys. Chem. A.* **107**, 140–147
18. Sikorska, E., Khmelinskii, I.V., Prukala, W., Williams, S.L., Patel, M., Worrall, D.R., Bourdelande, J.L., Koput, J., and Sikorski, M. (2004) Spectroscopy and photophysics of lumiflavins and lumichromes. *J. Phys. Chem. A.* **108**, 1501–1508
19. Hirst, J.D., Colella, K., and Gilbert, A.T.B. (2003) Electronic circular dichroism of proteins from first-principles calculations. *J. Phys. Chem. B.* **107**, 11813–11819
20. Frisch, M.J., Trucks, G.W., Schlegel, H.B., Scuseria, G.E., Robbins, D.J., Cheeseman, J.R., Montgomery, J.A.,Jr., Vreven, T., Kudin, K., Burant, J.C., Millam, J.M., Iyenger, S.S., Tomasi, J., Barone, V., Mennucci, B., Cossi, M., Scalmani, G., Rega, N., Petersson, G.A., Nakatsuji, H., Hada, M., Ehara, M., Toyota, K., Fukuda, R., Hasegawa, J., Ishida, M., Nakajima, T., Honda, Y., Kitao, O., Nakai, H., Klene, M., Li, X., Knox, J.E., Hratchian, H.P., Cross, J.B., Adamo, C., Jaramillo, J., Gomperts, R., Stratmann, R.E., Yazyev, O., Salvador, A., Dannenberg, J.J., Zakrzewski, V.G., Dapprich, S., Daniels, A.D., Strain, M.C., Farkas, O., Malick, D.K., Rabuck, A.D., Raghavachari, K., Foresman, J.B., Ortiz, J.V., Cui, Q., Baboul, A.G., Clifford, S., Cioslowski, J., Stefanov, B.B., Liu, G., Liashenko, A., Piskorz, P., Komaromi, I., Martin, R.L., Fox, D.J., Keith, T., Al-Laham, M.A., Peng, C.Y., Nanayakkara, A., Challacombe, M., Gill, P.M.W., Johnson, B., Chen, W., Wong, M.W., Gonzalez, C., Pople, J.A. (2003) Gaussian 03, Revision B.04, Gaussian, Inc., Pittsburgh, PA
21. Becke, A.D. (1993) Density-functional thermochemistry. III. The role of exact exchange. *J. Chem. Phys.* **98**, 5648–5652
22. Lee, C., Yang, W., Parr, R.G. (1988) Development of the Colle-Salvetti correlation-energy formula into a functional of the electron density. *Phys. Rev. B.* **37**, 785–789